EPR study of tetragonal and monoclinic Fe^{3+} centres in Rb_2ZnF_4 crystals

1991 J. Phys.: Condens. Matter 3 4405

(http://iopscience.iop.org/0953-8984/3/24/011)

J. Phys.: Condens. Matter 3 (1991) 4405–4420. Printed in the UK

EPR study of tetragonal and monoclinic Fe^{3+} centres in Rb_2ZnF_4 crystals

H Takeuchi†, M Arakawa‡ and H Ebisu‡

† Department of Physics, College of General Education, Nagoya University, Nagoya 464-01, Japan

‡ Department of Physics, Nagoya Institute of Technology, Nagoya 466, Japan

Received 25 February 1991

Abstract. EPR measurements have been made on tetragonal and monoclinic Fe^{3+} centres in Rb_2ZnF_4 at room temperatures. The fine-structure terms for the monoclinic centre are separated into uniaxial and cubic terms for comparison with the Fe^{3+}–V_K centre in $KZnF_3$ and for the uncompensated tetragonal centre. The monoclinic centre is ascribed to a Fe^{3+} ion associated with the nearest-Rb^+ vacancy and the principal z-axis is found to be 7° from the [001]-axis in the opposite direction to that of the Rb^+ vacancy. Rudowicz's NCC parameters for the monoclinic Fe^{3+} and Cr^{3+} centres are examined in relation to the separation of the spin-Hamiltonians. The calculated metal–ligand distances and deviation angles for the front and back fluorines by Newman's superposition model are in good agreement with, respectively, the distances for the uncompensated centre and angles for the Fe^{3+}–V_K centre in $KZnF_3$ determined from ^{19}F-ENDOR measurements. The relationships between the b_n^m and the axial and cubic parameters obtained by the superposition model are similar to those obtained from the spin-Hamiltonian separation.

1. Introduction

Many studies of electron paramagnetic resonance (EPR) have been devoted to understanding the local environments around substitutional magnetic ion sites in crystals using the fine-structure parameters b_n^m. As probe ions trivalent chromium, iron and gadolinium ions are superior to divalent vanadium, manganese or europium ions because of their large fine-structure and small hyperfine splittings (Aleksandrov *et al* 1985, Müller and Berlinger 1985, Vaills and Buzaré 1987, Arakawa *et al* 1988b). However, the identification of magnetic impurity centres with low symmetries, such as orthorhombic or monoclinic ones, from the values of b_n^m parameters are often difficult unless appropriate analyses are made on them.

As described in Abragam and Bleaney (1970, p 372), in traditional EPR studies the tetragonal and trigonal fine-structure terms in the spin-Hamiltonians for ions with $S \geq 2$ are separated analytically into uniaxial and cubic symmetry terms. In previous works (Takeuchi *et al* 1982, 1987b, Arakawa *et al* 1986, 1988a), we extended this analytical method to centres with orthorhombic symmetry up to the sixth-rank terms. We originally called the analytical method 'spin-Hamiltonian separation' when it was applied to fine-structure terms with symmetries lower than tetragonal or trigonal. Using spin-Hamiltonian separation we can separate the fine-structure terms for

0953-8984/91/244405+16$03.50

orthorhombic or monoclinic symmetries into several terms with strict uniaxial and cubic symmetries. In some cases where several relationships between the fine-structure parameters are assumed this can only be done approximately.

The spin-Hamiltonian separation method has the following aspects.

(1) It is useful to identify the magnetic impurity centres, especially charge-compensated centres with low symmetries, such as the Cr^{3+} centres in Cs_2CdCl_4 (Takeuchi and Arakawa 1983) where several ambiguities over the signs and directions of the principal-axes of the fine-structure terms were left in the original work by Kay and McPherson (1981). The signs of the fine-structure parameters obtained at high temperatures, where the depopulation effect cannot be used to determine the signs, can be deduced as described in this work, and the direction of a charge-compensator relative to those of the principal axes of the fine-structure terms can be obtained using spin-Hamiltonian separation. We also successfully separated the fine-structure terms of trivalent chromium and gadolinium centres in K_2NiF_4-like layered perovskite fluorides into uniaxial and cubic terms, where each uniaxial parameter was in good agreement with either one for the uncompensated centre in the same matrix crystal or one for the charge-compensated centre in cubic perovskite crystal.

(2) The good agreement between the axial parameters for the centre studied with those for the corresponding centres prompted us to use Newman's superposition model (hereafter denoted SPM). For a computer-fitting calculation of SPM analysis in sixfold-coordinated complexes, the number of accurately-determined fine-structure parameters is usually much less than the number of independent fitting parameters consisting of R_i, θ_i, ϕ_i $(i = 1, \ldots, 6)$. So, the computer-fitting calculation may not be successful without some model for the ligand configuration. Spin-Hamiltonian separation suggests a reasonable model of ligand configuration for SPM analysis.

(3) It does not make any assumptions such as the superposition of single ligand contributions or particular dependence of fine-structure parameters to metal–ligand distances as is made in SPM, although the result of spin-Hamiltonian separation can be derived within the framework of SPM when an appropriate ligand configuration is assumed.

(4) Recently, the formula for the rotational transformation properties of the extended Stevens operators was made available by Rudowicz (1985). This has enabled us to extend the spin-Hamiltonian separation method to the fourth- and sixth-rank fine-structure terms.

In the present work, we will report the results from EPR measurements for tetragonal and monoclinic Fe^{3+} centres in layered-perovskite Rb_2ZnF_4 crystals. In section 3.1, the tetragonal centre will be identified from the spectrum and spin-Hamiltonian parameters as the uncompensated Fe^{3+} centre. The field-direction dependence of the EPR spectrum from the monoclinic centre showed two maximum spreads with the greatest range for resonant magnetic field values along the directions with small tilt angles about $\pm 7°$ from the [001]-direction in the $(\bar{1}10)$-plane among all external field directions (section 3.2). For the identification of the monoclinic centre, we will apply spin-Hamiltonian separation to its fine-structure terms up to the fourth rank in section 4.1. Although the tilt angle of the principal z-axis is small compared with that of the Cr^{3+}–V_K centres in K_2ZnF_4 (Takeuchi *et al* 1982, Takeuchi 1983), the monoclinic centre will be identified as the Fe^{3+} centre associated with the nearest-Rb^+ vacancy. It will be found from the sign of the tilt angle that the principal z-axis is declined from the crystalline [001]-axis by about 7° in the opposite direction to the Rb^+ vacancy in contrast to the Cr^{3+}–V_K centres.

Recently, Rudowicz (1988a, 1988b, 1989) proposed a net-charge-compensation (NCC) model as an alternative to spin-Hamiltonian separation and applied it to the orthorhombic Cr^{3+} centres in layered perovskite fluorides. In section 4.2, the relationship between the Rudowicz's NCC model and that of spin-Hamiltonian separation will be discussed.

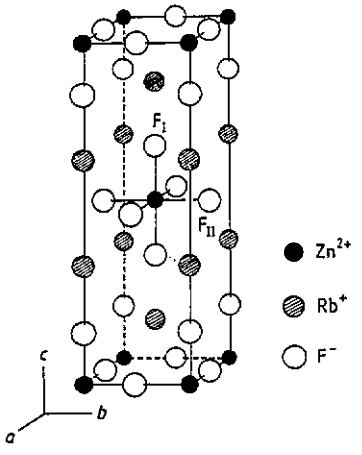

Figure 1. Unit cell of K_2NiF_4-like layered perovskite compounds.

The SPM was first proposed to explain the fine-structure parameters b_n^m determined by EPR measurements on rare-earth ions mostly in oxide crystals using assumed ligand configurations (Newman 1971, Newman and Urban 1975). It was later extended to the transition-metal ions, especially to $3d^5$ ions in oxides (Newman and Siegel 1976, Siegel and Müller 1979, Müller and Berlinger 1985). As for the transition-metal ions in fluoride crystals, several studies (Murrieta *et al* 1979, 1980) have reported SPM has been successfully applied to Fe^{3+} ions in perovskite fluorides. In a recent work (Takeuchi *et al* 1987a), we reported EPR results for tetragonal Fe^{3+} centres in cubic perovskite $RbCdF_3$ and $CsCdF_3$ crystals, where the fine-structure terms were analysed by SPM. From a simultaneous fitting of the second- and fourth-rank fine-structure parameters, we determined the metal–ligand distances and SPM parameters which are consistent with the previously reported values for the Fe^{3+} centres in perovskite fluorides by Murrieta *et al* (1980). For an examination of whether SPM parameters are applicable to other fluorides, the layered perovskite Rb_2ZnF_4 crystals are appropriate. It will be shown in section 4.3 that the separation of the monoclinic fine-structure terms in the spin-Hamiltonian separation analysis corresponds to the separation of the monoclinic ligand configuration in the SPM analysis. The metal–ligand distances and deviation angles for ligand fluorines will be calculated using the SPM. The results will be discussed in comparison with the electron–nuclear double resonance (ENDOR) data for the Fe^{3+}–V_K and the Cr^{3+}–V_K centres in $KZnF_3$ (Krebs and Jeck 1972, Takeuchi *et al* 1982, Takeuchi 1983) in section 5.

2. Experimental procedures

The Rb_2ZnF_4 crystal has a K_2NiF_4-like layered perovskite structure. The tetragonal unit cell with space group D_{4h}^{17} is shown in figure 1, where the fluorine octahedron is slightly distorted along the crystalline *c*-axis.

Single crystals doped with Fe^{3+} ions (about 1 mol%) were grown by the flux method using the Bridgman technique. Starting mixtures of RbF and ZnF_2 powders were heated to 900 °C to yield liquid mixtures under an argon atmosphere. Then the temperatures were lowered to 650 °C with a cooling rate of 10 °C h^{-1}. The crystals obtained were cleaved in the *c*-plane. The measurements were made at room temperatures using a JES-FE1XG ESR spectrometer operating in the X-band at the Centre for Instrumental Analysis at Nagoya Institute of Technology. The x-ray irradiations were performed using a Cu tube operating at 40 kV and 20 mA. The numerical computations were performed by the computer at the Computation Centre at Nagoya University.

3. Results

3.1. Tetragonal centre

The EPR spectrum observed from a tetragonal Fe^{3+} centre in Rb_2ZnF_4 shows the greatest spread in the [001]-direction and has a slight field-direction dependence with $\pi/2$ period in the (001)-plane (hereafter called centre I). The intensity of the signals enhanced by x-ray irradiation for about 20 h at room temperature as shown with mark I in figure 2, where the magnetic field is parallel to the [001]-axis. It was found by absorptiometry analysis that the as-grown crystal contains Fe^{2+} and Fe^{3+} ions in the ratio of about 2:1. The enhancement of the signals shows that some Fe^{2+} ions changed to Fe^{3+} ions.

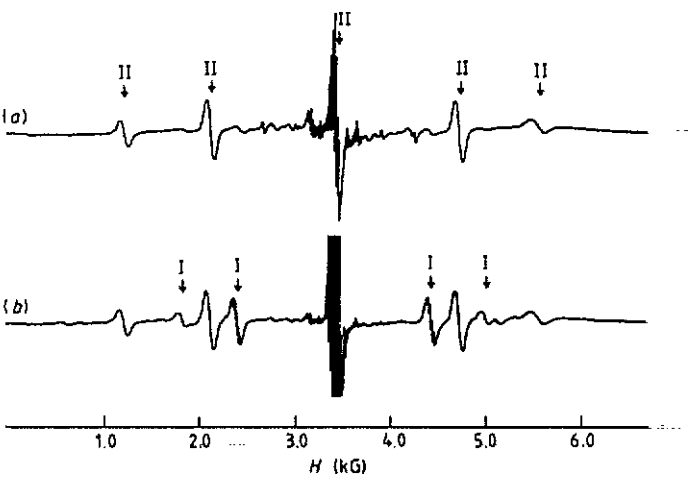

Figure 2. EPR spectra of the tetragonal (I) and monoclinic (II) Fe^{3+} centres in Rb_2ZnF_4 observed at 290 K with $H \parallel [001]$ from an as-grown crystal: (*a*) before x-ray irradiation and (*b*) after irradiation for about 20 h at room temperature.

The EPR spectra from Fe^{3+} centres can be described by the following spin-Hamiltonian:

$$\mathcal{H} = g_x\beta S_x H_x + g_y\beta S_y H_y + g_z\beta S_z H_z + \frac{1}{3}\sum_{m=0}^{2} b_2^m O_2^m + \frac{1}{60}\sum_{m=0}^{4} b_4^m O_4^m \qquad (1)$$

where the electronic spin $S = 5/2$ and β is Bohr magneton. The Stevens operators O_n^m with even m and O_4^3 are defined in Abragam and Bleaney (1970) and those with $m = 1$ are derived from the definition of extended Stevens operators by Rudowicz (1985) as follows:

$$O_2^1 = \{S_xS_z\}_S \qquad O_4^1 = \{S_x[7S_z^3 - \{1 + 3S(S+1)\}S_z]\}_S. \tag{2}$$

For centre I the x, y and z axes are chosen to be parallel to the crystalline a, b and c axes, respectively (hereafter called the (abc)-coordinate system). The spin-Hamiltonians with tetragonal symmetry including the terms with $m = 0$ and 4 only were fitted to the resonance fields using the direct matrix-diagonalization method on a computer. The values obtained for the parameters are listed in table 1.

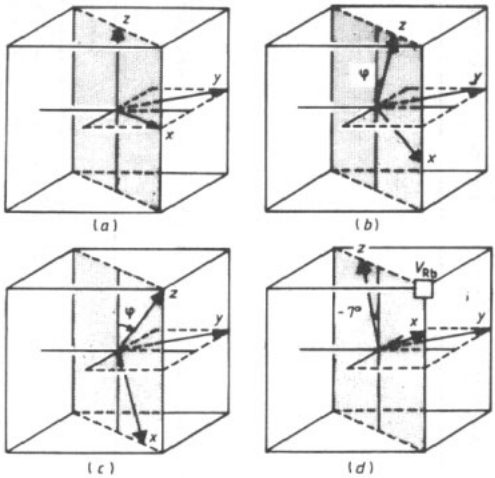

Figure 3. Coordinate systems (*a*) A, (*b*) B and (*c*) C in which the spin-Hamiltonians are described. (*d*) The configuration of the monoclinic Fe^{3+} centre in Rb_2ZnF_4 identified in the text and the coordinate systems with vanishing b_2^1.

By using the transformation properties of the Stevens operators shown by Rudowicz (1985), the equivalent operator $O_4^0 + 5O_4^4$ written in the (abc)-coordinate system can be transformed into the following form in the coordinate system B in figure 3(*b*):

$$\tfrac{1}{4}(15c^4 - 10c^2 - 1)O_4^0 + 10sc(3c^2 - 5)O_4^3 + (3c^2 - 1)[-10scO_4^1 + 5s^2O_4^2 + \tfrac{5}{4}(c^2 - 3)O_4^4]$$

where $c = \cos\varphi$ and $s = \sin\varphi$. Therefore, we can separate the fine-structure terms into uniaxial terms $(1/3)b_{2a}O_2^0$, $(1/60)b_{4a}O_4^0$ and a cubic term either $(1/60)b_{4c}(O_4^0 - 5O_4^4)$ for a tetragonal centre in the coordinate system A in figure 3(*a*) or $(1/60)b_{4c}[(-2/3)O_4^0 - (40\sqrt{2}/3)O_4^3]$ for a trigonal centre in the coordinate system C in figure 3(*c*). The axial and cubic parameters can be calculated as

$$b_{2a} = b_2^0 \qquad b_{4a} = b_4^0 - b_4^4/5 \qquad b_{4c} = b_4^4/5$$

for the tetragonal centre and

$$b_{2a} = b_2^0 \qquad b_{4a} = b_4^0 - b_4^3/(20\sqrt{2}) \qquad b_{4c} = (-3/40\sqrt{2})b_4^3$$

Table 1. Experimental values of the spin-Hamiltonian parameters for the Fe^{3+} centres in Rb_2ZnF_4 at 296 K. The parameters are given in the (*abc*)-coordinate system for the tetragonal centre (I) and in the coordinate system A for the monoclinic centre (II). Upper signs of b_n^m with odd m for the centre II are appropriate as mentioned in section 4.1. Units in 10^{-4} cm^{-1} for b_n^m.

Centre	g_x	g_y	g_z	b_2^0	b_2^1	b_2^2	b_4^0	b_4^1	b_4^2	b_4^3	b_4^4
Centre I	2.0035(5)	2.0035(5)	2.0026(5)	−403.3(2)	—	—	+29.7(1)	—	—	—	+121.5(5)
Centre II	2.006(1)	2.002(1)	2.003(1)	−543.5(5)	±449(5)	+185.5(5)	+27.8(3)	∓10(20)	−3(1)	∓90(60)	−103(1)

Table 2. Values of the uniaxial and cubic parameters for the centres I and II in Rb_2ZnF_4:Fe^{3+} and K_2ZnF_4:Cr^{3+} and the values for the V_K-associated centres in $KZnF_3$. Units in 10^{-4} cm^{-1}.

Ion	Crystal	Centre	$b_{2a(1)}$	$b_{2a(2)}$	$b_{4a(1)}$	$b_{4a(2)}$	b_{4c}	Symmetry	Reference
Fe^{3+}	Rb_2ZnF_4	Centre II	−543.5	+185.5	+7.2	−1.35	+20.08	Monoclinic	Present work
	Rb_2ZnF_4	Centre I	−403.3	—	+5.4	—	+24.30	Tetragonal	Present work
	$KZnF_3$	Fe^{3+}–V_K	—	+103.4	—	−1.30	+22.80	Trigonal	Krebs and Jeck (1972)
Cr^{3+}	K_2ZnF_4	Centre II	−591.3	−1572.7	—	—	—	Monoclinic	Takeuchi *et al* (1982)[a]
	K_2ZnF_4	Centre I	−381	—	—	—	—	Tetragonal	Takeuchi *et al* (1982)
	$KZnF_3$	Cr^{3+}–V_K	—	−1613	—	—	—	Trigonal	Patel *et al* (1976)

[a] Recalculated from the values obtained by direct-matrix diagonalization.

for the trigonal centre. We select a positive sign for b_{4c} for centre I in the same way as that used for the cubic Fe^{3+} centre in $KZnF_3$ ($b_4 = +26.35 \times 10^{-4}$ cm^{-1}) in Jeck and Krebs (1972). By this selection the signs of b_n^m for centre I are determined uniquely as listed in table 1. The calculated values of the axial ($b_{na}, n = 2, 4$) and cubic (b_{4c}) parameters for centre I are listed in table 2 together with the values for the trigonal Fe^{3+}–V_K centre in cubic perovskite $KZnF_3$. The parameters obtained for centre I in Rb_2ZnF_4 have values similar to those for the tetragonal Fe^{3+}–V_{Cd} centre in cubic perovskite $RbCdF_3$ reported in Takeuchi *et al* (1987a). However the signs for b_{na} are opposite to those for the trigonal Fe^{3+}–V_K centre in cubic perovskite $KZnF_3$. All three centres have similar values for b_{4c} and the ratios $b_{4a}/b_{2a}(\simeq -0.013$ to $-0.014)$.

From symmetry and the values obtained for the parameters, centre I may be identified as the uncompensated Fe^{3+} centre where the Fe^{3+} ion is substituted for a Zn^{2+} ion and is not associated with any charge compensators in its immediate neighbourhood.

3.2. Monoclinic centre

In some Rb_2ZnF_4:Fe^{3+} crystals a spectrum from a Fe^{3+} centre with monoclinic symmetry C_{1h} was observed (hereafter called centre II) as shown in figure 2. When the magnetic field is parallel to the [001]-direction, the total spread of the spectrum is larger than that for centre I. Each signal is split further when the magnetic field is rotated from the [001]-direction. The field-direction dependence of the highest-field line on magnetic field in the ($\bar{1}10$)-plane is shown in figure 4. Two branches, marked a_1 and a_2, have peaks with tilt angles about $\pm 7°$ away from the [001]-direction, respectively. In these directions the spread of the spectrum shows the greatest range of resonant magnetic field values among all external field directions. The branch marked b has a peak in the [001]-direction. The field-direction dependence on the magnetic field in the (001)-plane is shown in figure 5, where the spectrum with period π shows maximum and minimum spreads in this plane in the [110]- and [$\bar{1}$10]-directions, respectively, and a crossover in the [010]-direction, although the maximum spread of the spectrum is smaller than that for the [001]-direction.

As the spectrum shows the greatest spread in the field direction near the [001]-axis in the ($\bar{1}10$)-plane, we describe the spectrum in the coordinate system A with the z- and x-axes in the symmetry plane. Considering the features of this spectrum, we fit it by a spin-Hamiltonian with monoclinic fine-structure terms where all possible $m(\geq 0)$ appear. The off-diagonal Zeeman term is omitted. The optimum parameters obtained are listed in table 1. As the parameter b_4^4 for a cubic centre is negative in the coordinate system A, we choose a negative sign for b_4^4 for centre II which gives uniquely the signs of parameters b_n^m with even m. We must be careful to fit the parameters b_n^m with odd m in the coordinate system A because their signs are fitted independently of those with even m, although the relative signs of b_n^m within odd m can be uniquely determined. The signs of parameters b_n^m with odd m will be determined using spin-Hamiltonian separation in the following section.

4. Analyses

4.1. Spin-Hamiltonian separation for centre II

The appearance of the spectrum shown in figure 4 with small tilt angles of $\pm 7°$ is similar to that for the low-temperature phase of K_2CdF_4: Cr^{3+} previously reported

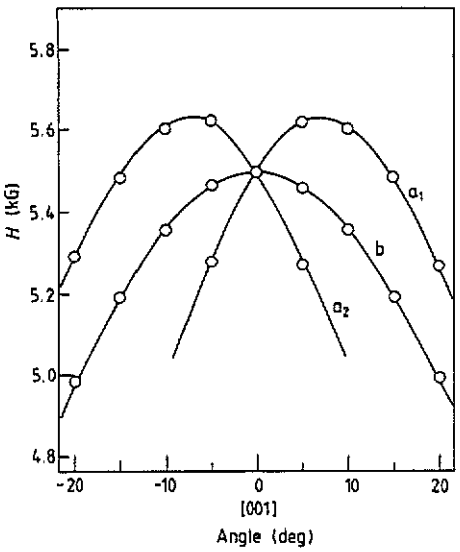

Figure 4. Field-direction dependence of the highest-field line for the monoclinic Fe^{3+} centre (centre II) about the [001]-axis with H in the $(\bar{1}10)$-plane. Full curves are calculated using the spin-Hamiltonian parameters listed in table 1.

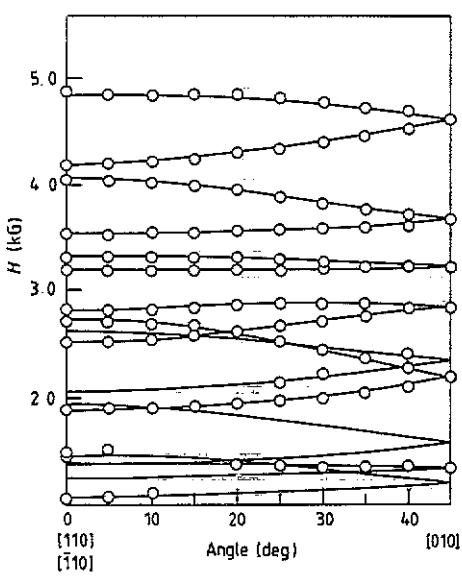

Figure 5. Field-direction dependence of the monoclinic Fe^{3+} centre with H in the (001)-plane. Full curves are calculated using the spin-Hamiltonian parameters listed in table 1.

(Arakawa *et al* 1988b). However, in the present crystal, the possibility of structural phase transition producing low symmetry in the matrix crystal is excluded by the existence of centre I at the temperature investigated. So, the spectrum of centre II suggests the existence of some kind of charge-compensator in the $(\bar{1}10)$- or (110)-plane in the tetragonal phase of the matrix crystal. Identifying centre II with the greatest

spread in the direction close to the [001]-axis may be difficult to attain instantly from the fine-structure parameters obtained unless they are analysed further.

Here, we apply spin-Hamiltonian separation by assuming the existence of the nearest-Rb^+ vacancy in the $(\bar{1}10)$- or (110)-plane as a charge compensator. We try to separate the monoclinic fine-structure terms into: a cubic term; uniaxial terms with parameters $b_{2a(1)}, b_{4a(1)}$ along the crystalline [001]-axis; and ones with parameters $b_{2a(2)}, b_{4a(2)}$ along the z-axis of the coordinate system C. Then, the fine-structure terms for centre II described in the coordinate system A can be separated as follows:

$$\frac{1}{3}\sum_{m=0}^{2} b_2^m O_2^m + \frac{1}{60}\sum_{m=0}^{4} b_4^m O_4^m = \frac{1}{3}[b_{2a(1)}O_2^0 + b_{2a(2)}O_{2(2)}^0] + \frac{1}{60}[b_{4a(1)}O_4^0 + b_{4a(2)}O_{4(2)}^0] + \frac{1}{60}b_{4c}[O_4^0 - 5O_4^4] \tag{3}$$

where $O_{n(2)}^m$ are the Stevens operators denoted in coordinate system C. Equation (3) is valid when the following conditions are satisfied:

$$\begin{aligned} b_{2a(1)} &= b_2^0 \qquad b_{2a(2)} = b_2^2 \qquad b_{4a(1)} = b_4^0 + \tfrac{1}{5}b_4^4 \\ b_{4a(2)} &= \tfrac{9}{20}b_4^2 \qquad b_{4c} = \tfrac{1}{40}(7b_4^2 - 8b_4^4) \end{aligned} \tag{4}$$

for even m and

$$b_{2a(2)} = \frac{1}{2\sqrt{2}}b_2^1 \qquad b_{4a(2)} = -\frac{9}{10\sqrt{2}}b_4^1 \qquad b_{4a(2)} = \frac{9}{70\sqrt{2}}b_4^3 \tag{5}$$

for odd m. Since the fine-structure terms with eight fine-structure parameters b_n^m are roughly expressed by the terms with only five new parameters, three relationships—$b_2^1 = 2\sqrt{2}b_2^2$ and $b_4^2 = -\sqrt{2}b_4^1 = (\sqrt{2}/7)b_4^3$—are assumed, although the experimental relative errors are very large for b_4^1, b_4^2 and b_4^3. Hereafter in the discussion we use the parameters b_n^m with even m and b_2^1, as these have small experimental relative errors except for small b_4^2. In table 2, the values of $b_{na(1)}, b_{na(2)}$ and b_{4c} calculated by equation (4) are listed together with the values of the related Fe^{3+} centres. As for the Cr^{3+}–V_K centre in K_2ZnF_4 (Takeuchi *et al* 1982), each value of the parameters has the same sign and a similar magnitude to that for the corresponding centre. From these results the monoclinic Fe^{3+} centre in Rb_2ZnF_4 may be identified as a nearest-Rb^+-vacancy associated centre.

As seen from table 2, the positive sign for b_{4c} shows that the selection of a negative sign for b_4^4 made in the preceding section was correct. As for the signs of b_n^m with odd m, the positive b_2^1 gives a positive value for the ratio $b_2^1/b_2^2 = +2.7$, and negative b_2^1 gives a negative one. Since the positive value is almost same as the value $2\sqrt{2}(\simeq +2.8)$ expected from equations (4) and (5), a positive b_2^1 is reasonable. So, the absolute signs of b_n^m with odd m can be determined as the upper signs in table 1.

Spin-Hamiltonian separation can describe the small tilt angles of the direction where the spectrum shows the greatest spread. Using the transformation properties of the Stevens operators given by Rudowicz (1985), we can transform the second-rank fine-structure terms $(\frac{1}{3})\sum b_2^m O_2^m$ described in the coordinate system A into ones described in the coordinate system B where the term $(\frac{1}{3})b_2^1 O_2^1$ vanishes. The following

relationship must be satisfied among the tilt angle φ and the parameter b_n^m in the coordinate system A:

$$\tan 2\varphi = \frac{b_2^1}{3b_2^0 - b_2^2}. \tag{6}$$

Since $3b_2^0 - b_2^2 < 0$ and $b_2^1 > 0$ as previously determined, the angle φ should be negative. The second-rank spin-Hamiltonian parameters and the tilt angle determined in the coordinate system B with vanishing b_2^1 are as follows:

$$b_2^0 = -557.0(5) \times 10^{-4}\ \text{cm}^{-1} \qquad b_2^2 = +199.0 \times 10^{-4}\ \text{cm}^{-1} \qquad \varphi = -6.92(4)^\circ.$$

The result indicates that the direction where the spectrum shows the greatest spread is declined away from the [001]-axis by a small angle of about 7° toward the *opposite* direction to the Rb^+ vacancy as shown in figure 3(*d*).

Since the spin-Hamiltonian for the Cr^{3+}–V_K centre in K_2ZnF_4 was analysed by the use of the perturbation method in the previous work (Takeuchi *et al* 1982), we determine the spin-Hamiltonian parameters more accurately by direct matrix-diagonalization method. The results are as follows:

$$g_x = 1.9744(2) \qquad g_y = 1.9737(4) \qquad g_z = 1.9721(2)$$

$$b_2^0 = -1874.5(5) \times 10^{-4}\ \text{cm}^{-1} \qquad b_2^2 = -289.5(5) \times 10^{-4}\ \text{cm}^{-1} \qquad \varphi = +43.92(5)^\circ.$$

From these values for the Cr^{3+} centre we can obtain the values of b_2^0, b_2^1 and b_2^2 in the coordinate system A by the use of the rotational properties of O_2^m. The parameters $b_{2a(1)}$ and $b_{2a(2)}$ are listed in table 2. The agreement of these with those of the corresponding centres is also good in the monoclinic Cr^{3+} centre. The contrast features of φ for the Fe^{3+} and Cr^{3+} ions will be discussed in relation to the ratio $b_{2a(1)}/b_{2a(2)}$ in section 5.

4.2. Relationship of the NCC model with spin-Hamiltonian separation

Rudowicz (1988a, 1988b, 1989) proposed a net-charge-compensation (NCC) model to describe the net effect of a charge compensator on the fine-structure terms in only one coordinate system. We have already reported on the relationship between the NCC parameters and spin-Hamiltonian separation for orthorhombic Cr^{3+} and Gd^{3+} centres (Takeuchi *et al* 1987b, Arakawa *et al* 1988a). Here, we show the relationship between the monoclinic Fe^{3+} and Cr^{3+} centres.

In the NCC model the difference between the fine-structure terms for the monoclinic centre (II) and ones for the uncompensated centre (I) can be expressed as follows:

$$\sum_m b_n^m O_n^m - \sum_m b_n^m(\mathrm{I}) O_n^m = \sum_m b_n'^m \{O_n^m\} \tag{7}$$

where O_n^m and $\{O_n^m\}$ are the Stevens operators denoted in the coordinate systems A and C, respectively; and $b_n^m(\mathrm{I})$ are the parameters for centre I. Then, the second-rank NCC parameters $b_2'^m$ are given by the following relationships:

$$b_2'^0 = b_{2a(2)} - \tfrac{2}{3}d_{2a(2)} \qquad b_2'^1 = -2\sqrt{2}[d_{2a(1)} - \tfrac{1}{3}d_{2a(2)}] \qquad b_2'^2 = d_{2a(1)} + \tfrac{2}{3}d_{2a(2)} \tag{8}$$

where

$$d_{2a(1)} = b_{2a(1)} - b_2^0(\mathrm{I}) \qquad d_{2a(2)} = b_2^2 - \frac{1}{2\sqrt{2}} b_2^1. \tag{9}$$

The parameter $d_{2a(1)}$ represents the deviation of the uniaxial parameter for centre II from that for centre I due to the relaxation effect caused by the charge compensator. The parameter $d_{2a(2)}$ represents the deviation of centre II from the spin-Hamiltonian separation scheme as it vanishes when the relation $b_2^1/b_2^2 = 2\sqrt{2}$ is strictly satisfied. Each contribution from $b_{2a(2)}$, $d_{2a(1)}$ and $d_{2a(2)}$ must be examined separately in the discussion of NCC parameters. The calculated values of $b_2'^m$ are listed in table 3. Each contribution from $d_{2a(1)}$ in $b_2'^1$ or $b_2'^2$ for the Cr^{3+} centre is larger than that for the Fe^{3+} centre and suggests the existence of a larger relaxation effect for the Cr^{3+} centre by the charge compensator. The contributions from $d_{2a(2)}$ are less in the Fe^{3+} centre relative to those in the Cr^{3+} centre, where they are comparable with the contributions from $d_{2a(1)}$. It can be explained from table 3 that the separated parameters $b_{2a(2)}$ for the Fe^{3+} and Cr^{3+} ions have similar values to those for the corrresponding trigonal centres in spite of the large magnitudes of the NCC parameters $b_2'^1$, as the contribution to $b_2'^0$ from $b_{2a(2)}$ is dominant.

Table 3. Values of the second-rank NCC parameters $b_2'^m$ for Rb_2ZnF_4:Fe^{3+}–V_{Rb} and K_2ZnF_4:Cr^{3+}–V_K centres. Units in 10^{-4} cm^{-1}.

	$b_{2a(2)}$	Term in $d_{2a(1)}$	Term in $d_{2a(2)}$	Total
Rb_2ZnF_4:Fe^{3+}–V_{Cd}				
$b_2'^0$	+185.5	—	−17.9	+167.7
$b_2'^1$	—	+396.5	+25.3	+421.8
$b_2'^2$	—	−140.2	+17.9	−122.3
K_2ZnF_4:Cr^{3+}–V_K				
$b_2'^0$	−1572.7	—	−207.9	−1780.6
$b_2'^1$	—	+594.8	+294.0	+888.8
$b_2'^2$	—	−210.3	+207.9	−2.4

4.3. SPM calculations for ligand configurations

As mentioned in section 4.1, it is found by spin-Hamiltonian separation analysis that the tetragonal and monoclinic centres are, respectively, the uncompensated and V_{Rb}-associated substitutional Fe^{3+} centres. Furthermore, the axial parameters of centre II are in good agreement with those of the corresponding centres. These results prompt us to try the SPM analysis for these centres, and suggest reasonable ligand configurations for both centres.

Previously, from EPR and ^{19}F-ENDOR results we considered that the local environment of the Cr^{3+}–V_K centres in K_2ZnF_4 and K_2MgF_4 may be explained by the ligand configuration shown in figure 4 in Takeuchi *et al* (1982), where each ligand deviates in the planes of the perovskite cell in a direction opposite to that of the K^+ vacancy. We assume a similar configuration C_1 for the FeF_6 cluster in the Fe^{3+}–V_{Rb} centre as shown in figure 6(*a*), where the metal–ligand distances are R_1 for F^I ions and R_2

for F^{II} ions and the deviation angles are α for the front fluorines (numbered 1, 2, 3) and β for back fluorines (4, 5, 6). The related configurations C_2, C_3, C_4 shown in figures 6(*b*), (*c*), and (*d*) have environments similar to centre I in Rb_2ZnF_4 and the V_K-associated centre and cubic centre in $KZnF_3$, respectively.

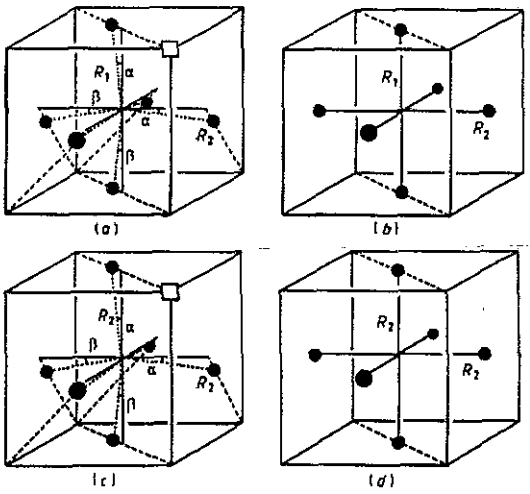

Figure 6. (*a*) Assumed configuration C_1 for the Fe^{3+}–V_{Rb} centre in Rb_2ZnF_4 and related (*b*) tetragonal C_2, (*c*) trigonal C_3 and (*d*) cubic C_4 configurations.

Table 4. The numerical factors p_j and q_j defined in equation (12).

Parameter	p_1	p_2	p_3	p_4	p_5	q_1	q_2	q_3	q_4	q_5
b_2^0	2	—	−3/2	—	—	—	—	—	—	—
b_2^1	—	−6	—	—	—	—	−12	$3\sqrt{2}$	—	—
b_2^2	—	—	3/2	—	—	—	$-3\sqrt{2}$	3/2	—	—
b_4^0	2	—	−5	—	35/8	7/2	—	−35/4	—	105/16
b_4^1	—	−20	—	35	—	—	−5	$-15\sqrt{2}/2$	35/2	$35\sqrt{2}/4$
b_4^2	—	—	15	—	−35/2	—	$5\sqrt{2}$	15	$-35\sqrt{2}/2$	−35/2
b_4^3	—	—	—	−35	—	—	35	$105\sqrt{2}/2$	−245/2	$-245\sqrt{2}/4$
b_4^4	—	—	—	—	35/8	−35/2	—	175/4	—	−525/16

In SPM, the spin-Hamiltonian parameters b_n^m are assumed to be calculated:

$$b_n^m = \sum_{i=1}^{6} \bar{b}_n(R_i) K_n^m(\theta_i, \phi_i) \tag{10}$$

where $K_n^m(\theta_i, \phi_i)$ are the coordination factors for the ith ligands with polar coordinates (R_i, θ_i, ϕ_i). Furthermore, the intrinsic parameters $\bar{b}_n(R_i)$ are assumed to be expressed by a single-exponential law:

$$\bar{b}_n(R_i) = \bar{b}_n(R_0)\left(\frac{R_0}{R_i}\right)^{t_n} \tag{11}$$

where R_0 denotes the reference distances. Then, the fine-structure parameters b_n^m for the present monoclinic configuration C_1 are expressed in the SPM as follows:

$$b_n^m = \sum_{j=1}^{5} f_j(\alpha,\beta)\{p_j[\bar{b}_n(R_1) - \bar{b}_n(R_2)] + q_j\bar{b}_n(R_2)\} \tag{12}$$

where the functions $f_j(\alpha,\beta)$ are defined as

$$\begin{aligned} &f_1(\alpha,\beta) = 1 \qquad f_2(\alpha,\beta) = \cos\alpha\sin\alpha - \cos\beta\sin\beta \\ &f_3(\alpha,\beta) = \sin^2\alpha + \sin^2\beta \qquad f_4(\alpha,\beta) = \cos\alpha\sin^3\alpha - \cos\beta\sin^3\beta \\ &f_5(\alpha,\beta) = \sin^4\alpha + \sin^4\beta. \end{aligned} \tag{13}$$

The numerical factors p_j and q_j are listed in table 4. When $\alpha = \beta = 0$ in equation (12), we obtain the expressions for the tetragonal configuration C_2, where the axial terms result from radial distortion of the fluorine octahedron. When $R_1 = R_2$ in equation (12), we obtain the expressions for the trigonal configuration C_3, where the axial terms result from angular distortion of the fluorine octahedron. The expression for the cubic configuration C_4 is obtained when $\alpha = \beta = 0$ and all distances are R_2. When we denote the parameters for the configurations C_1, C_2, C_3, C_4 by b_n^m, $b_n^m(C_2)$, $b_n^m(C_3)$, $b_n^m(C_4)$, respectively, in the coordinate system A, the following relationships hold:

$$b_n^m = b_n^m(C_2) + b_n^m(C_3) - b_n^m(C_4) + \sum_{j=2}^{5} p_j f_j(\alpha,\beta)[\bar{b}_n(R_1) - \bar{b}_n(R_2)]. \tag{14}$$

The third term represents the cancellation out of the cubic expression from C_2, as other cubic expression appears from C_3. The terms in the summation are cross terms of radial and angular distortions, and have the orders of

$$\bar{b}_n(R_0)\cdot t_n(\alpha-\beta)(R_2-R_1)/R_0 \qquad \text{or} \qquad \bar{b}_n(R_0)\cdot t_n(\alpha^2+\beta^2)(R_2-R_1)/R_0$$

or higher for small α and β as the expansions

$$\bar{b}_n(R_1) - \bar{b}_n(R_2) \simeq \bar{b}_n(R_0)\cdot t_n(R_2-R_1)/R_0$$

hold for small $(R_2-R_1)/R_0$. They are much smaller than the dominant terms $b_n^m(C_2)$ or $b_n^m(C_3)$. Thus, the monoclinic configuration C_1 is obtained by removing the cubic configuration C_4 from the superposition of tetragonal C_2 and trigonal C_3 configurations in the approximation where the small radial-angular cross terms are neglected. When we define the parameters as

$$\begin{aligned} b_{na(1)} &= 2[\bar{b}_n(R_1) - \bar{b}_n(R_2)] \\ b_{2a(2)} &= -\tfrac{3}{2}[2\sqrt{2}f_2 - f_3]\bar{b}_2(R_2) \\ b_{4a(2)} &= \tfrac{9}{8}[2\sqrt{2}f_2 + 6f_3 - 7\sqrt{2}f_4 - 7f_5]\bar{b}_4(R_2) \\ b_{4c} &= \frac{7}{2}\left[1 + \frac{\sqrt{2}}{4}f_2 - \frac{7}{4}f_3 - \frac{7\sqrt{2}}{8}f_4 + f_5\right]\bar{b}_4(R_2) \end{aligned} \tag{15}$$

and neglect the radial-angular cross terms, relationships similar to equations (4) and (5) obtained by spin-Hamiltonian separation analysis are derived again within the framework of SPM.

Here, we calculate the values R_1, R_2, α and β for centres II and I in Rb_2ZnF_4 and V_K-associated centre in $KZnF_3$ assuming their configurations to be C_1, C_2 and C_3, respectively. In order to estimate the distances and angles, we use the following values for the intrinsic parameters and power-law exponents for the common reference distance $R_0 = 1.950$ A for $n = 2$ and 4 calculated from the values of equation (9) in Takeuchi *et al* (1987):

$$\begin{aligned} \bar{b}_2(R_0) &= (-1160 \pm 70) \times 10^{-4}\ \mathrm{cm}^{-1} \qquad t_2 = 8.0 \pm 0.2 \\ \bar{b}_4(R_0) &= (+8.4 \pm 1.1) \times 10^{-4}\ \mathrm{cm}^{-1} \qquad t_4 = 14.0 \pm 0.5. \end{aligned} \tag{16}$$

The results are listed in table 5.

Table 5. Calculated values of R_1, R_2, α, β and b_n^m using the SPM. Coordinate systems are A, (*abc*) and C for the centre II, centre I in Rb_2ZnF_4 and Fe^{3+}-V_K centre in $KZnF_3$, respectively. Units in Å for distances, deg for angles and 10^{-4} cm^{-1} for b_n^m.

Centre	R_1	R_2	α	β	b_2^0	b_2^1	b_2^2	b_4^0	b_4^3	b_4^4
Rb_2ZnF_4:centre II										
Cal	1.934	1.994	2.9	0.5	−536	+499	+154	+27.8	—	−107
Exp	—	—	—	—	−543.5	+449	+185.5	+27.8	—	−103
Rb_2ZnF_4:centre I										
Cal	1.933	1.976	—	—	−403	—	—	+29.4	—	+122
Exp	—	—	—	—	−403.3	—	—	+29.7	—	+121.5
$KZnF_3$:Fe^{3+}–V_K										
Cal	1.981	1.981	2.9	1.5	+103	—	—	−15	−444	—
Cal[a]	—	—	—	—	+106	—	—	−13	−378[c]	—
Exp[b]	—	—	—	—	+103.4	—	—	−16.5	−429.9	—

[a] Murrieta *et al* (1980).
[b] Krebs and Jeck (1972).
[c] The sign of b_4^3 is changed from that in Murrieta *et al* (1980) as the coordinate system is rotated from their one about the z-axis by an angle π.

5. Discussions

In A_2MF_4 crystals two monovalent cations exist along the [001]- and [00$\bar{1}$]-directions around a M^{2+} site in place of the divalent cations in contrast to cubic perovskite crystals AMF_3. The tetragonal symmetry of the crystal structure may be reflected in the relaxed configuration of ligand fluorines in the uncompensated impurity centres. As seen from table 5, the SPM analysis of the fine-structure terms for centre I shows the tetragonal compression of the ligand octahedron along the c-axis. So, in the V_{Rb}-assocated centre in Rb_2ZnF_4, it may be expected that a compression along the c-axis will be added to the trigonally-distorted ligand octahedron. In section 4.1, we successfully separated the monoclinic fine-structure terms into terms with tetragonal, trigonal and cubic symmetries. The separated parameters are in good agreement with those of the corresponding centres.

As seen from table 2, the parameters $b_{2a(1)}$ for both the monoclinic Fe^{3+} centre in Rb_2ZnF_4 and the monoclinic Cr^{3+} centre in K_2ZnF_4 have negative signs and similar magnitudes. In contrast to $b_{2a(1)}$, $b_{2a(2)}$ and the deviation angle φ for the Fe^{3+} centre have different magnitudes and inverse signs compared with those for the Cr^{3+} centres, where the principal z-axis is close to the direction to the K^+-vacancy ($\varphi = 43.92°$). As the direction of the principal z-axis is related to the ratio $b_{2a(1)}/b_{2a(2)}$ (Takeuchi *et al* 1982), it can be explained by spin-Hamiltonian separation that the small negative tilt angle ($\varphi = -6.92°$) for the Fe^{3+} centre is due to the small positive $b_{2a(2)}$.

By the ^{19}F-ENDOR measurement for the Cr^{3+}–V_K centre in K_2ZnF_4 the deviation angles have been determined to be $\alpha = 8.7°$ for the front fluorines and $\beta = 3.0°$ for the back fluorines (Takeuchi *et al* 1982). For the trigonal Fe^{3+}–V_K centre in $KZnF_3$ the deviation angles were determined from the ^{19}F-ENDOR measurements by Krebs and Jeck (1972) as $\alpha = 2.8°$ and $\beta = 1.1°$ which is small compared with those of the Cr^{3+} centre. Murrieta *et al* (1980) calculated the fine-structure terms for the trigonal Fe^{3+}–V_K centres in $KZnF_3$ and $KMgF_3$ by SPM, assuming a model where the fluorines deviate in the planes of the perovskite unit cell of host crystals. From our refined calculation where the metal–ligand distances R_1 and R_2 are fitted independently to the deviation angles in SPM analysis, the deviation angles for the Fe^{3+}–V_K centre in $KZnF_3$ were obtained to be: $\alpha = 2.9°$ and $\beta = 1.5°$; in good agreement with the ENDOR results for this centre. The deviation angles $\alpha = 2.9°$ and $\beta = 0.5°$ for the Fe^{3+}–V_{Rb} centre in Rb_2ZnF_4 obtained by SPM analysis may be reasonable as they are close to the values for the Fe^{3+}–V_K centre in $KZnF_3$.

6. Conclusions

Centre I with tetragonal symmetry about the c-axis has been identified as the uncompensated Fe^{3+} centre. Centre II with monoclinic symmetry is identified to be the substitutional Fe^{3+} centre associated with a nearest Rb^+-vacancy using spin-Hamiltonian separation. The signs of φ and b_n^m with odd m are determined by spin-Hamiltonian separation. It is found from these parameters that the direction where the spectrum of the monoclinic centre shows the greatest spread is declined away from the [001]-axis by a small angle of about 7° in a direction opposite to that of the Rb^+ vacancy. Rudowicz's NCC parameters $b_2'^m$ for the monoclinic centres contain two contributions from relaxation effects in $d_{2a(1)}$ by the charge compensator and deviation from spin-Hamiltonian separation scheme in $d_{2a(2)}$, except for the contributions from the parameters $b_{2a(2)}$. It is suggested from larger contributions in $d_{2a(1)}$ that the Cr^{3+}–V_K centre in K_2ZnF_4 are more affected by the charge compensator compared with the Fe^{3+}–V_{Rb} centre in Rb_2ZnF_4. The metal–ligand distances and deviation angles of ligand fluorines are calculated by the use of superposition model. The distances and angles obtained are consistent with the corresponding centres and in good agreement with the ^{19}F-ENDOR data reported for the Fe^{3+}–V_K centres in $KZnF_3$. The expressions for the assumed monoclinic configuration are separated into the tetragonal, trigonal and cubic configurations in the approximation where the small radial-angular cross terms are neglected. The relationships between the uniaxial and cubic parameters and b_n^m are also derived from the SPM analysis in the same approximation.

Acknowledgments

The authors appreciate and thank Dr T Uchida for the concentration analysis of iron ions by absorptiometry, and Dr M Mori for his help in x-ray irradiation and for useful discussions.

References

Abragam A and Bleaney B 1970 *Electron Paramagnetic Resonance of Transition Ions* (Oxford: Clarendon Press)
Aleksandrov K S, Emelyanova L S, Misjul S V and Kokov I T 1985 *Solid State Commun.* **53** 835–9
Arakawa M, Ebisu H and Takeuchi H 1986 *J. Phys. Soc. Japan* **55** 2853–8
—— 1988a *J. Phys. Soc. Japan* **57** 2801–4
—— 1988b *J. Phys. Soc. Japan* **57** 3573–9
Jeck R K and Krebs J J 1972 *Phys. Rev.* B **5** 1677–87
Kay D and McPherson G L 1981 *J. Phys. C: Solid State Phys.* **14** 3247–53
Krebs J J and Jeck R K 1972 *Phys. Rev.* B **5** 3499–505
Müller K A and Berlinger W 1985 *Phys. Rev.* B **32** 5837–44
Murrieta H S, Lopez F J and Rubio J O 1980 *J. Phys. Soc. Japan* **49** 499–503
Murrieta H S, Rubio J O and Aguilar G S 1979 *Phys. Rev.* B **19** 5516–24
Newman D J 1971 *Adv. Phys.* **20** 197–256
Newman D J and Siegel E 1976 *J. Phys. Soc. Japan* **9** 4285–92
Newman D J and Urban W 1975 *Adv. Phys.* **24** 793–844
Patel J L, Davies J J, Cavenett C, Takeuchi H and Horai K 1976 *J. Phys. C: Solid State Phys.* **9** 129–38
Rudowicz C 1985 *J. Phys. C: Solid State Phys.* **18** 1415–30
—— 1988a *Phys. Rev.* B **37** 27–34
—— 1988b *Solid State Commun.* **65** 631–5
Rudowicz C, Misra S K and Bramley R 1989 *Magnetic Resonance and Related Phenomena* ed Stankowski *et al* (Amsterdam: Elsevier) pp 621–33
Siegel E and Müller K A 1979 *Phys. Rev.* B **20** 3587–96
Takeuchi H 1983 *Research Bulletin, College General Education Nagoya University* B **27** 41–9
Takeuchi H and Arakawa M 1983 *J. Phys. Soc. Japan* **52** 279–83
Takeuchi H, Arakawa M, Aoki H, Yosida T and Horai K 1982 *J. Phys. Soc. Japan* **51** 3166–72
Takeuchi H, Arakawa M and Ebisu H 1987a *J. Phys. Soc. Japan* **56** 3677–82
—— 1987b *J. Phys. Soc. Japan* **56** 4571–80 [Errata 1990 **59** 2297]
Vaills Y and Buzaré J Y 1987 *J. Phys. C: Solid State Phys.* **20** 2149–59